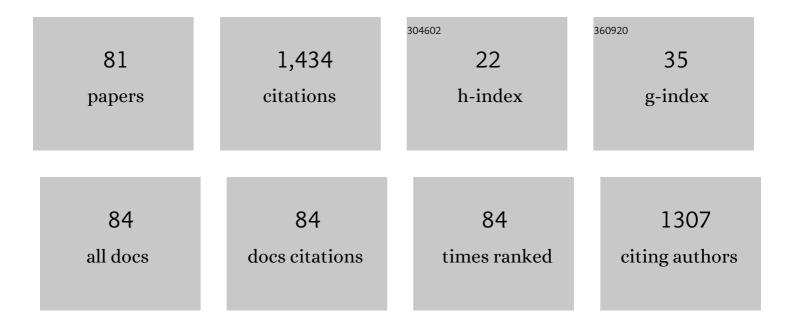
## Tae-Hyuk Kwon

List of Publications by Year in descending order

Source: https://exaly.com/author-pdf/3166730/publications.pdf Version: 2024-02-01



TAE-HYLIK KWON

#	Article	IF	CITATIONS
1	Entrapment of clay particles enhances durability of bacterial biofilm-associated bioclogging in sand. Acta Geotechnica, 2022, 17, 119-129.	2.9	4
2	Effect of Salt Water on the Process of Microbially Induced Carbonate Precipitation. , 2022, , .		1
3	Grain-Scale Tensile and Shear Strengths of Glass Beads Cemented by MICP. Journal of Geotechnical and Geoenvironmental Engineering - ASCE, 2022, 148, .	1.5	9
4	Sensitivity analysis of influencing parameters on slit-type barrier performance against debris flow using 3D-based numerical approach. International Journal of Sediment Research, 2021, 36, 50-62.	1.8	5
5	Assessment of barrier location effect on debris flow based on smoothed particle hydrodynamics (SPH) simulation on 3D terrains. Landslides, 2021, 18, 217-234.	2.7	23
6	Preliminary report of a catastrophic landslide that occurred in Gokseong County, South Jeolla Province, South Korea, on August 7, 2020. Landslides, 2021, 18, 1465-1469.	2.7	7
7	Relaxation behavior in low-frequency complex conductivity of sands caused by bacterial growth and biofilm formation by <i>Shewanella oneidensis</i> under a high-salinity condition. Geophysics, 2021, 86, B389-B400.	1.4	4
8	A Newly Developed State-of-the-Art Full-Scale Excavation Testing Apparatus for Tunnel Boring Machine (TBM). KSCE Journal of Civil Engineering, 2021, 25, 4856-4867.	0.9	5
9	Effect of Soft Viscoelastic Biopolymer on the Undrained Shear Behavior of Loose Sands. Journal of Geotechnical and Geoenvironmental Engineering - ASCE, 2021, 147, .	1.5	4
10	Auto-detection of acoustic emission signals from cracking of concrete structures using convolutional neural networks: Upscaling from specimen. Expert Systems With Applications, 2021, 186, 115863.	4.4	15
11	A Case Study on the Closed-Type Barrier Effect on Debris Flows at Mt. Woomyeon, Korea in 2011 via a Numerical Approach. Energies, 2021, 14, 7890.	1.6	1
12	Fines migration and pore clogging induced by single- and two-phase fluid flows in porous media: From the perspectives of particle detachment and particle-level forces. Geomechanics for Energy and the Environment, 2020, 23, 100131.	1.2	28
13	Photoelastic observation of toughness-dominant hydraulic fracture propagation across an orthogonal discontinuity in soft, viscoelastic layered formations. International Journal of Rock Mechanics and Minings Sciences, 2020, 134, 104438.	2.6	17
14	Microbiology and Microbial Products for Enhanced Oil Recovery. , 2020, , 27-65.		4
15	Theory and Experiments. , 2020, , 67-108.		1
16	Modeling and Simulation. , 2020, , 109-168.		0
17	An Integrated Approach to Real-Time Acoustic Emission Damage Source Localization in Piled Raft Foundations. Applied Sciences (Switzerland), 2020, 10, 8727.	1.3	7
18	Long-Term Remote Monitoring of Ground Deformation Using Sentinel-1 Interferometric Synthetic Aperture Radar (InSAR): Applications and Insights into Geotechnical Engineering Practices. Applied Sciences (Switzerland), 2020, 10, 7447.	1.3	18

ΤΑΕ-ΗΥΝΚ ΚΌΟΝ

#	Article	IF	CITATIONS
19	Study on Viscous Fluid Flow in Disordered-Deformable Porous Media Using Hydro-mechanically Coupled Pore-Network Modeling. Transport in Porous Media, 2020, 133, 207-227.	1.2	6
20	Review on geotechnical engineering properties of sands treated by microbially induced calcium carbonate precipitation (MICP) and biopolymers. Construction and Building Materials, 2020, 246, 118415.	3.2	155
21	Surface-erosion behaviour of biopolymer-treated soils assessed by EFA. Geotechnique Letters, 2020, 10, 106-112.	0.6	45
22	Effect of Fluid–Rock Interactions on In Situ Bacterial Alteration of Interfacial Properties and Wettability of CO <sub>2</sub> –Brine–Mineral Systems for Geologic Carbon Storage. Environmental Science & Technology, 2020, 54, 15355-15365.	4.6	11
23	Fluid-driven mechanical responses of deformable porous media during two-phase flows: Hele-Shaw experiments and hydro-mechanically coupled pore network modeling. E3S Web of Conferences, 2020, 205, 08009.	0.2	Ο
24	Video data of hydraulic fracture propagation in two-dimensionally confined gelatin plates. Data in Brief, 2019, 25, 104096.	0.5	1
25	Characteristics of steady-state propagation of hydraulic fractures in ductile elastic and two-dimensionally confined plate media. International Journal of Rock Mechanics and Minings Sciences, 2019, 114, 164-174.	2.6	9
26	The Production-Induced Geomechanical Property Changes during Gas Production from Gas Hydrate Deposits. , 2019, , .		0
27	Impact of Interbedded Structure of Sand and Clay Layers on Geomechanical Responses of Hydrate-Bearing Sediments During Depressurization. , 2019, , .		Ο
28	Modification of Interfacial Tension and Wettability in Oil–Brine–Quartz System by in Situ Bacterial Biosurfactant Production at Reservoir Conditions: Implications for Microbial Enhanced Oil Recovery. Energy & Fuels, 2019, 33, 4909-4920.	2.5	30
29	Xâ€Ray Computed Microtomography Imaging of Abiotic Carbonate Precipitation in Porous Media From a Supersaturated Solution: Insights Into Effect of CO <sub>2</sub> Mineral Trapping on Permeability. Water Resources Research, 2019, 55, 3835-3855.	1.7	16
30	Systematic Modeling Approach to Selective Plugging Using <i>In Situ</i> Bacterial Biopolymer Production and Its Potential for Microbial-enhanced Oil Recovery. Geomicrobiology Journal, 2019, 36, 468-481.	1.0	19
31	Study of Korea Early Warning System for Slope Failure. Korean Society of Hazard Mitigation, 2019, 19, 73-81.	0.1	2
32	Numerical Computation of Hydraulic Conductivity of Sand Using X-ray Microtomography Imaging of a Pore Structure. Korean Society of Hazard Mitigation, 2019, 19, 187-192.	0.1	0
33	Depressurizationâ€Induced Fines Migration in Sediments Containing Methane Hydrate: Xâ€Ray Computed Tomography Imaging Experiments. Journal of Geophysical Research: Solid Earth, 2018, 123, 2539-2558.	1.4	42
34	Effect of Electric Field on Gas Hydrate Nucleation Kinetics: Evidence for the Enhanced Kinetics of Hydrate Nucleation by Negatively Charged Clay Surfaces. Environmental Science & Technology, 2018, 52, 3267-3274.	4.6	48
35	Modeling of Permeability Reduction in Bioclogged Porous Sediments. Journal of Geotechnical and Geoenvironmental Engineering - ASCE, 2018, 144, .	1.5	14
36	Improvement of Surface Erosion Resistance of Sand by Microbial Biopolymer Formation. Journal of Geotechnical and Geoenvironmental Engineering - ASCE, 2018, 144, .	1.5	65

ΤΑΕ-ΗΥΝΚ ΚΌΟΝ

#	Article	IF	CITATIONS
37	Effect of Pore Size Distribution on Dissociation Temperature Depression and Phase Boundary Shift of Gas Hydrate in Various Fine-Grained Sediments. Energy & Fuels, 2018, 32, 5321-5330.	2.5	38
38	Effects of bacterial dextran on soil geophysical properties. Environmental Geotechnics, 2018, 5, 114-122.	1.3	8
39	Effect of slit-type barrier on characteristics of water-dominant debris flows: small-scale physical modeling. Landslides, 2018, 15, 111-122.	2.7	31
40	Microbial community analyses of produced waters from highâ€ŧemperature oil reservoirs reveal unexpected similarity between geographically distant oil reservoirs. Microbial Biotechnology, 2018, 11, 788-796.	2.0	31
41	Effect of Moisture Content and Particle Size on Extinction Coefficients of Soils Using Terahertz Time-Domain Spectroscopy. IEEE Transactions on Terahertz Science and Technology, 2017, 7, 529-535.	2.0	13
42	Visualization and prediction of supercritical CO2 distribution in sandstones during drainage: An in situ synchrotron X-ray micro-computed tomography study. International Journal of Greenhouse Gas Control, 2017, 66, 230-245.	2.3	21
43	Hydromechanical responses of coal powders by CO2 adsorption. Environmental Geotechnics, 2017, 4, 94-102.	1.3	1
44	Biosurfactant as an Enhancer of Geologic Carbon Storage: Microbial Modification of Interfacial Tension and Contact Angle in Carbon dioxide/Water/Quartz Systems. Frontiers in Microbiology, 2017, 8, 1285.	1.5	15
45	The emerging role of 4D synchrotron X-ray micro-tomography for climate and fossil energy studies: five experiments showing the present capabilities atÂbeamline 8.3.2 at the Advanced Light Source. Journal of Synchrotron Radiation, 2017, 24, 1237-1249.	1.0	10
46	In situ viscoelastic properties of insoluble and porous polysaccharide biopolymer dextran produced by Leuconostoc mesenteroides using particle-tracking microrheology. Geomechanics and Engineering, 2017, 12, 849-862.	0.9	5
47	Measuring elastic modulus of bacterial biofilms in a liquid phase using atomic force microscopy. Geomechanics and Engineering, 2017, 12, 863-870.	0.9	7
48	Use of a Pre-Drilled Hole for Implementing Thermal Needle Probe Method for Soils and Rocks. Energies, 2016, 9, 846.	1.6	5
49	Geomechanical, Hydraulic and Thermal Characteristics of Deep Oceanic Sandy Sediments Recovered during the Second Ulleung Basin Gas Hydrate Expedition. Energies, 2016, 9, 775.	1.6	18
50	Roles of spacing and angle of slit-type barriers on velocity reduction of debris flows. Japanese Geotechnical Society Special Publication, 2016, 2, 963-966.	0.2	0
51	Preliminary study on P-wave monitoring of soil erosion in SRICOS-EFA method. Japanese Geotechnical Society Special Publication, 2016, 2, 1757-1760.	0.2	0
52	Analysis of laboratory data on ultrasonic monitoring of permeability reduction due to biopolymer formation in unconsolidated granular media. Geophysical Prospecting, 2016, 64, 445-455.	1.0	1
53	<i>P</i> and <i>S</i> wave responses of bacterial biopolymer formation in unconsolidated porous media. Journal of Geophysical Research G: Biogeosciences, 2016, 121, 1158-1177.	1.3	26
54	Observation of the Degradation Characteristics and Scale of Unevenness on Three-dimensional Artificial Rock Joint Surfaces Subjected to Shear. Rock Mechanics and Rock Engineering, 2016, 49, 3-17.	2.6	38

ΤΑΕ-ΗΥΝΚ ΚΌΟΝ

#	Article	IF	CITATIONS
55	Experimental investigation on the variation of thermal conductivity of soils with effective stress, porosity, and water saturation. Geomechanics and Engineering, 2016, 11, 771-785.	0.9	10
56	Ultrasonic P-Wave Reflection Monitoring of Soil Erosion for Erosion Function Apparatus. Geotechnical Testing Journal, 2016, 39, 301-314.	0.5	15
57	Interactions between hydraulic fracture and interfaces in layered formations. , 2016, , 217-221.		Ο
58	A small pore size effect on dissociation behavior of gas hydrates in fine-grained sediments. , 2016, , 459-462.		1
59	Observations of poreâ€scale growth patterns of carbon dioxide hydrate using <scp>X</scp> â€ray computed microtomography. Geochemistry, Geophysics, Geosystems, 2015, 16, 912-924.	1.0	55
60	Rheological Properties of Cemented Tailing Backfill and the Construction of a Prediction Model. Materials, 2015, 8, 2076-2092.	1.3	25
61	Preliminary Study of Geophysical Monitoring of Bioclogging Caused by Bacterial Biopolymer Accumulation in Sands. , 2014, , .		1
62	Diffusive and Convective Transport of Disposed CO <sub>2</sub> in Porous Media: A Numerical Approach. , 2014, , .		1
63	Site characterization and geotechnical aspects on geological storage of CO2 in Korea. Geosciences Journal, 2014, 18, 167-179.	0.6	20
64	Geomechanical and Thermal Responses of Hydrate-Bearing Sediments Subjected to Thermal Stimulation: Physical Modeling Using a Geotechnical Centrifuge. Energy & Fuels, 2013, 27, 4507-4522.	2.5	29
65	Effect of CO <sub>2</sub> hydrate formation on seismic wave velocities of fineâ€grained sediments. Geochemistry, Geophysics, Geosystems, 2013, 14, 1787-1799.	1.0	14
66	High-frequency seismic response during permeability reduction due to biopolymer clogging in unconsolidated porous media. Geophysics, 2013, 78, EN117-EN127.	1.4	27
67	Submarine Slope Failure Primed and Triggered by Bottom Water Warming in Oceanic Hydrate-Bearing Deposits. Energies, 2012, 5, 2849-2873.	1.6	28
68	Thermal Dissociation Behavior and Dissociation Enthalpies of Methane–Carbon Dioxide Mixed Hydrates. Journal of Physical Chemistry B, 2011, 115, 8169-8175.	1.2	29
69	Geotechnical properties of deep oceanic sediments recovered from the hydrate occurrence regions in the Ulleung Basin, East Sea, offshore Korea. Marine and Petroleum Geology, 2011, 28, 1870-1883.	1.5	61
70	Effect of Partial Water Saturation on Attenuation Characteristics of Low Porosity Rocks. Rock Mechanics and Rock Engineering, 2011, 44, 245-251.	2.6	11
71	Seismic monitoring of permeability reduction due to biopolymer formation in unconsolidated materials. , 2011, , .		3
72	An experimental procedure for evaluating the consolidation state of marine clay deposits using shear wave velocity. Smart Structures and Systems, 2011, 7, 289-302.	1.9	4

ΤΑΕ-ΗΥϤΚ Κ₩ΟΝ

#	Article	IF	CITATIONS
73	Shear behavior of rectangular-shaped asperities in rock joints. KSCE Journal of Civil Engineering, 2010, 14, 323-332.	0.9	29
74	Destabilization of Marine Gas Hydrate-Bearing Sediments Induced by a Hot Wellbore: A Numerical Approach. Energy & Fuels, 2010, 24, 5493-5507.	2.5	33
75	Evolution of Compressional Wave Velocity during CO <sub>2</sub> Hydrate Formation in Sediments. Energy & Fuels, 2009, 23, 5731-5736.	2.5	15
76	Gas hydrate dissociation in sediments: Pressureâ€ŧemperature evolution. Geochemistry, Geophysics, Geosystems, 2008, 9, .	1.0	100
77	Dissociation Behavior of CO <sub>2</sub> Hydrate in Sediments during Isochoric Heating. Environmental Science & Technology, 2008, 42, 8571-8577.	4.6	18
78	MONITORING OF CO2 HYDRATE FORMATION IN SEDIMENTS USING COMPRESSIONAL WAVE VELOCITY. , 2008, , .		0
79	Smart geophysical characterization of particulate materials in a laboratory. Smart Structures and Systems, 2005, 1, 217-233.	1.9	9
80	Characterization of soil properties using elastic and electromagnetic waves. , 2003, 5057, 440.		0
81	Monitoring of Low-Frequency Seismic Responses during Microbial Biofilm and EPS Formations in Unconsolidated Sediments. Environmental Geotechnics, 0, , 1-10.	1.3	2